THE ASTROPHYSICAL JOURNAL, 320:159–177, 1987 September 1

PHYSICAL PARAMETERS FOR 12 PLANETARY NEBULAE AND THEIR CENTRAL STARS IN THE MAGELLANIC CLOUDS

LAWRENCE H. ALLER[1] AND CHARLES D. KEYES
Department of Astronomy, University of California, Los Angeles

AND

STEPHEN P. MARAN,[1] THEODORE R. GULL,[1] ANDREW G. MICHALITSIANOS,[1] AND THEODORE P. STECHER[1]
Laboratory for Astronomy and Solar Physics, NASA/Goddard Space Flight Center
Received 1986 October 20; accepted 1987 February 27

ABSTRACT

Nebular and central star parameters and elemental abundances of C, N, O, Ne, S, and Ar are presented for the planetary nebulae, N2, N5, N43, N44, N54, and N67 in the Small Magellanic Cloud and P2, P7, P9, P25, P33, and P40 in the Large Magellanic Cloud, which were observed with the *IUE*. Here N denotes the number in Henize's catalog (1956) and P the number in the Westerlund and Smith (1964) listing. The nebular chemical compositions are affected by nuclear processes in the precursor stars. The precursors may not have been sufficiently massive to synthesize Ne, S, or Ar, which appear to be deficient with respect to their solar abundances by factors of roughly 4 and 5 for the LMC and SMC, respectively. Even excluding nebulae formed by stars in which O apparently was destroyed by nuclear processes, O depletion in the LMC and SMC nebulae is significantly greater than in galactic planetaries. The estimated masses of the 12 remnant central stars range from 0.58 to 0.71 $M_\odot$; this includes three stars for which we previously derived masses close to 1 $M_\odot$ (Stecher *et al.* 1982). The change in estimated masses is due primarily to the adoption of non–LTE atmospheres that better represent the emergent flux distributions of the remnant stars than those used previously.

Subject headings: galaxies: Magellanic Clouds — nebulae: abundances — nebulae: planetary — ultraviolet: spectra

I. INTRODUCTION

This paper summarizes the results of analyses of ultraviolet spectrophotometry of 12 planetary nebulae in the Magellanic Clouds as obtained with the *International Ultraviolet Explorer* since 1981 May. Preliminary results on three of the nebulae, SMC N2, SMC N5, and LMC P40, were presented in Maran *et al.* (1982) and Stecher *et al.* (1982). In the present paper, we have been able to obtain more reliable parameters for these three nebulae and their central stars as well as for the additional objects thanks to the adoption of recently published model atmospheres (Husfeld *et al.* 1984) that appear to represent better the emergent flux distributions of the nebular central stars than do the models that were available at the time of our earlier work.

II. OBSERVATIONS

Table 1 lists the objects included in the present study. Column (1) gives the nebular designations. For the Small Magellanic Cloud (SMC), we have used the Henize (1956) designations, N2, N5, etc.; for the Large Magellanic Cloud (LMC), we use those of Westerlund and Smith (1964), P2, P7, etc. Other designations of these nebulae are given in column (7). Columns (2) and (3) give their positions for the epoch 1950. Column (4) gives the logarithm of the adopted Hβ flux (in units of ergs cm^{-2} s^{-1}). For the SMC, the flux data are from Webster (1969); for the LMC, they are adopted from Webster (1969) and Aller (1983), except for SMC N67 where the data for both flux and extinction are from Osmer (1976). Columns (5) and (6) give the visual and ultraviolet interstellar extinction, respectively, as defined below.

[1] Guest Observer, *International Ultraviolet Explorer*.

The Magellanic Cloud planetaries are all extremely faint; not surprisingly, none of the targets of this investigation is visible in images obtained with the *IUE* Fine Error Sensor (FES). Accordingly, the spectroscopic observations had to be obtained by guiding with the FES on an offset star, and it was necessary to have precise information on the right ascension and declination differentials between each target and the corresponding offset star. We obtained this information from PDS microdensitometer measurements of the coordinates of the nebulae and various reference and offset stars on plates of the ESO–SRC Southern Sky Atlas. The nebular coordinates for SMC N2, N5, and LMC P40 are taken from Maran *et al.* (1982).

All the *IUE* observations were made with the low-dispersion cameras and large entrance apertures (10″ × 20″). Thanks to the large distance of the Magellanic Clouds, the planetaries are effectively stellar in appearance, so that each nebular image at the focal plane of the telescope is contained wholly within the entrance aperture, and a monochromatic image of any of the planetaries as formed by an *IUE* spectrograph falls on a single 3″ detector pixel. Table 2 lists the *IUE* observations that were used to derive the results presented in the subsequent sections.

We corrected the measurements both for the *IUE* flux calibration and for interstellar extinction. Some of the reduced scans are shown in Figures 1, 2, 3 and 4. We observed He II λ1640 in all objects except N43, N44, and N54. For the nebulae showing λ1640 we determined the extinction constant $C = -\log F_{\rm OBSD}(\mathrm{H}\beta)/I_{\rm CORR}(\mathrm{H}\beta)$ from a comparison of the fluxes in He II λ4686 and λ1640 using Seaton's (1978) theoretical intensity ratio for these two lines for the adopted T_e. The thus determined extinctions are listed in Table 1, column (6), and denoted as $C_{\rm UV}$. We can obtain also an estimate of the extinction from

TABLE 1

PLANETARY NEBULAE INCLUDED IN PRESENT STUDY

OBJECT (1)	RIGHT ASCENSION (1950.0) (2)	DECLINATION (1950.0) (3)	ADOPTED $F(H\beta)$ (4)	ADOPTED C_{VIS} (5)	ADOPTED C_{UV} (6)	OTHER DESIGNATIONS (7)
SMC N2	$00^h30^m33^s.13$	$-71°58'32''.1$	−12.79	0.12	0.010	Ln 14, Mg 2
SMC N5	00 39 26.02	−73 01 43.2	−12.83	0.0	0.127	Ln 32, Mg 5
SMC N43	00 49 24.91	−74 13 53.7	−12.42	0.08	...	Ln 174, Mg 15
SMC N44	00 50 06.6	−71 41 00	−12.52	0.00	...	Ln 191, Mg 17
SMC N54	00 54 16.4	−70 35 39	−12.48	0.06	...	Ln 289, Mg 20
SMC N67	00 56 53.81	−71 51 58.9	−12.88	0.16	0.082	Ln 333, Mg 22
LMC P2	04 48 27.08	−72 33 27.9	−12.73	0.4	0.20	N 184, Mg 6, LM 4
LMC P7	05 05 04.83	−68 43 06.8	−12.78	0.2	0.15	N 97, LM 16, Mg 21
LMC P9	05 08 17.71	−68 43 58.9	−12.72	0.0	0.22	N 102, LM 19, Mg 29
LMC P25	05 25 39.60	−71 35 25.1	−12.31	0.3	0.20	N 201, LM 38, Mg 6
LMC P33	05 34 40.74	−69 00 15.2	−12.59	0.4	0.27	N 78, LM 49, Mg 78
LMC P40	06 10 36.56	−67 55 33.7	−12.88	(0.05)	0.13	LM 61, Mg 97

the Balmer decrement, C_{VIS}, which is listed in column (5). Visual wavelength region spectrophotometry (Aller *et al.* 1981; Aller 1983; Dufour and Killen 1977; Maran *et al.* 1982; Osmer 1976) was used both to investigate extinction effects and as input data needed for the nebular model calculations. Differences between C_{VIS} and C_{UV} for the same nebula are to be attributed to errors in measured Balmer or helium line intensities, uncertainties in the response functions, and, for the ground-based observations, uncertainties in atmospheric extinction. In the visual region we assumed the extinction to follow the Seaton (1979) function but corrected the ultraviolet fluxes for extinction using data by Nandy *et al.* (1981) for the LMC and by Hutchings (1982) for the SMC. Despite the similarity of the visual region extinction functions for the Galaxy and the Magellanic Clouds, there are differences in the ultraviolet which must be taken into account (Tables 3 and 4). The f_λ functions based on the data of Nandy *et al.* (1981) and of Hutchings (1982) are analogous to that defined by Seaton (1979).

TABLE 2

JOURNAL OF OBSERVATIONS

Object	Sequence No.	Date	Exposure (min.)
SMC N2	SWP 14078	1981 May 26	129
	SWP 20454	1983 Jul 14	100
	SWP 20527	1983 Jul 29	90
	LWR 10715	1981 May 26	37
SMC N5	SWP 14076	1981 May 26	180
	SWP 14077	1981 May 26	45
	SWP 20453	1983 Jul 14	80
SMC N43	SWP 20455	1983 Jul 14	33
	SWP 23415	1984 Jul 6	55
SMC N44	SWP 22775	1984 Apr 17	40
SMC N54	SWP 22767	1984 Apr 16	72
	SWP 22776	1984 Apr 17	35
SMC N67	SWP 22765	1984 Apr 16	45
	SWP 22766	1984 Apr 16	240
	LWP 3168	1984 Apr 17	266
LMC P2	SWP 20421	1983 Jul 9	150
	SWP 20422	1983 Jul 9	45
LMC P7	SWP 23397	1984 Jul 4	60
	SWP 23413	1984 Jul 6	120
LMC P9	SWP 20423	1983 Jul 9	30
	SWP 20424	1983 Jul 9	72
	LWR 16472	1983 Jul 29	120
LMC P25	SWP 23394	1984 Jul 4	45
	SWP 23414	1984 Jul 6	120
LMC P33	SWP 20528	1983 Jul 29	70
LMC P40	SWP 14032	1981 May 23	320
	SWP 14033	1981 May 23	30
	SWP 14074	1981 May 26	90
	SWP 20452	1983 Jul 14	90
	SWP 20592	1983 Aug 3	420
	LWR 10683	1981 May 23	47
	LWR 10684	1981 May 23	30
	LWR 10712	1983 May 26	240

Tables 3 and 4 give the measured and corrected UV fluxes for all nebulae in the LMC and SMC, respectively. For N43 and N54, only a single line, λ1909, C III], was measured with $F = 7.0 \times 10^{-13}$ ergs cm^{-2} s^{-1} (N43), $F = 1.59 \times 10^{-12}$ ergs cm^{-2} s^{-1} (N54). For N44 the extinction is taken as zero, while for N54 we chose $C = 0.06$. Then $F_{CORR}(1909) = 1.88(-12)$ in same units for N54.

If we express fluxes in units of 10^{-13} ergs cm^{-2} s^{-1}, the internal agreement of individual measurements suggests errors of the order of 30%–40% for fluxes less than 1, of the order of 20% for fluxes in the range 1–2 and 5%–15% for stronger lines. In converting from fluxes to intensities, small errors in C can lead to large uncertainties. When C_{UV} is determined from the 1640/4686 ratio, we are basically referring UV intensities to the He II λ1640 line and the final values should be trustworthy, but when λ1640 is not observed (as in N43 and in N54) and reliance must be placed on the Balmer decrement, uncertainties can be larger. Consequently, the carbon abundance in N43 will be poorly established, mostly because the extinction correction is very uncertain.

III. INTERPRETATION OF THE OBSERVATIONS

Magellanic Cloud planetaries are so very faint that only the strongest lines can be measured with the *IUE* and these only in the low-resolution mode. Ultraviolet region diagnostics suitable for bright objects are not available here. We obtain T_e from the usual [O III] or [N II] ratios from ground-based measurements. Electron density estimates are often very uncertain. The [S II] ratio may apply primarily to knots and condensations and may not yield good average N_e values. The remarkable technique recently applied by Barlow (1985) promises to yield valuable clues and further results are eagerly awaited. We are indebted to Michael Barlow, who supplied in advance of publication electron density estimates for our SMC planetaries and for P02, P07, P09, P44, and P54 in the LMC.

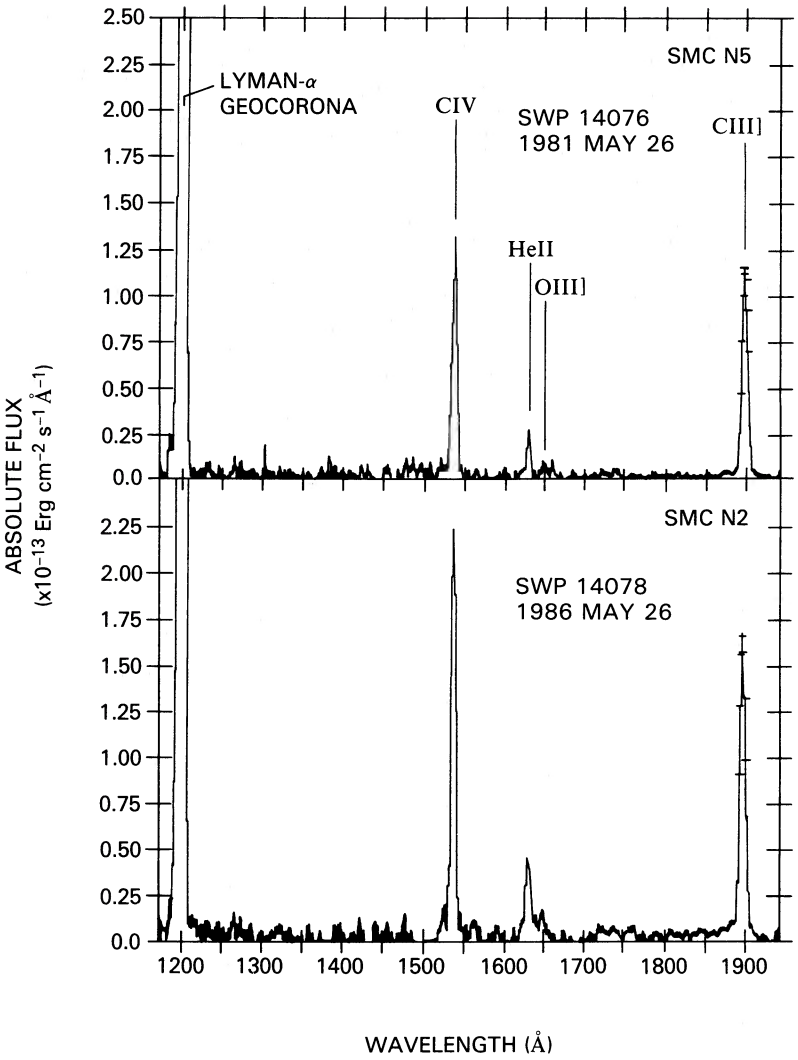

FIG. 1.—Spectra of SMC N2 and N5. Note the great strength of C III and C IV. The observed intensity of the He II λ1640 line is used in conjunction with that of λ4686 to evaluate the interstellar extinction using the theoretical intensity ratios by Seaton (1978).

TABLE 3

OBSERVED UV FLUXES AND CORRECTED INTENSITIES FOR LARGE MAGELLANIC CLOUD PLANETARIES

ION	WAVELENGTH (λ)	f_λ	P02		P07		P09		P25		P33		P40	
			F^a	I^a	F	I	F	I	F	I	F	I	F	I
N V	1238.8, 1242.8 1397.2	2.76	...	...	0.32	0.83	0.664	2.63	0.12	0.44	0.19:	1.06	<0.027	<0.062
O IV	1399.8, 1401.1 1404.8, 1407.4	2.16	...	...	0.11	0.232	...	...	0.13	0.36	...	...	<0.077	<0.15
N IV	1486.5	1.96	...	...	0.32	0.63	0.51	1.35	0.10	0.25	...	...	<0.071	<0.13
C IV	1548.2, 1550.7	1.86	1.33	3.13	0.34	0.646	0.355	0.915	0.36	0.87	0.23	0.73	1.59	2.77
He II	1640.3	1.64	0.186	0.396	0.37	0.65	0.40	0.922	0.38	0.82	0.19	0.53	0.41	0.67
O III]	1660.8, 1666.2 1746.8	1.60	0.145	0.303	0.17	0.295	0.164	0.37	0.13	0.28	0.073:	0.20	0.068	0.11
N III]	1748.6, 1749.7 1752.2, 1759.0	1.57	...	...	0.28	0.48	0.38	0.844	0.12	0.25				
C III]	1906.8, 1909.7	1.40	1.03	1.97	0.30	0.49	0.395	0.808	0.27	0.52	0.86	2.05	0.91	1.45
Ne IV	2426	1.04	...	...	...	...	0.122	0.208	...	...	...	...	0.106	0.161
C(UV) ...			0.20	...	0.15	...	0.22	...	0.205	...	0.27	...	0.13	...

[a] The measured flux F and corrected intensity I are given in units of 10^{-12} ergs cm^{-2} s^{-1}.

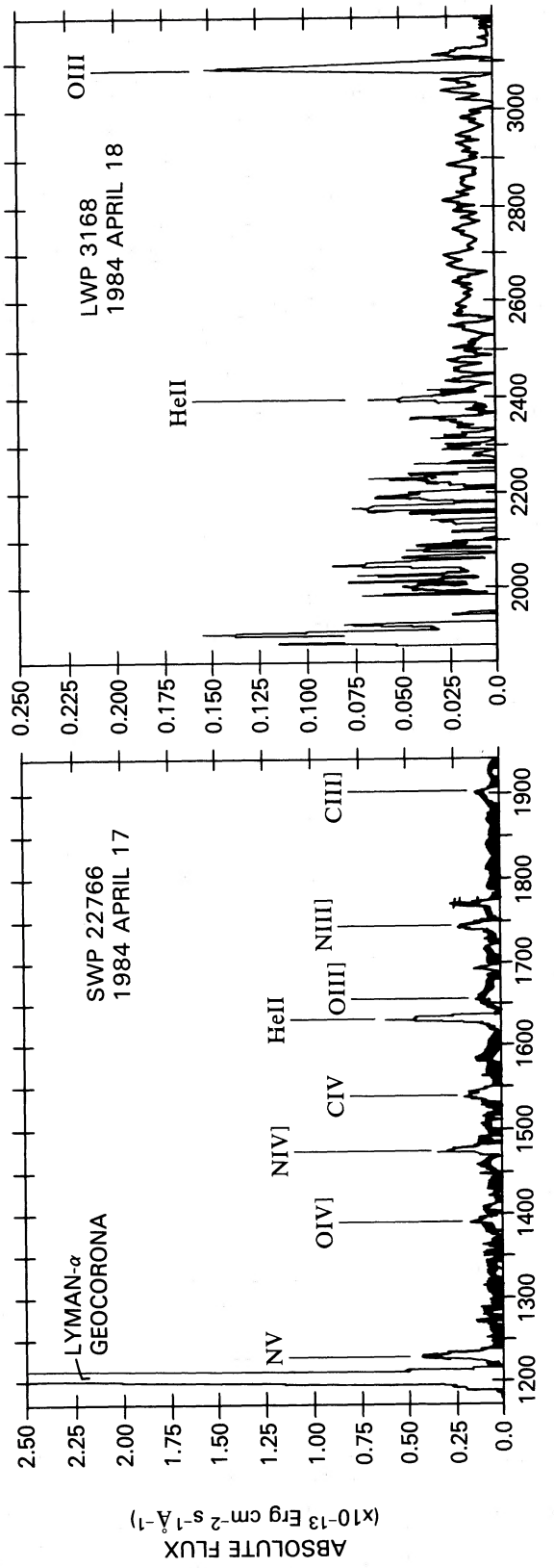

FIG. 2.—Spectrum of SMC N67. Notice the prominence of nitrogen ions in this object.

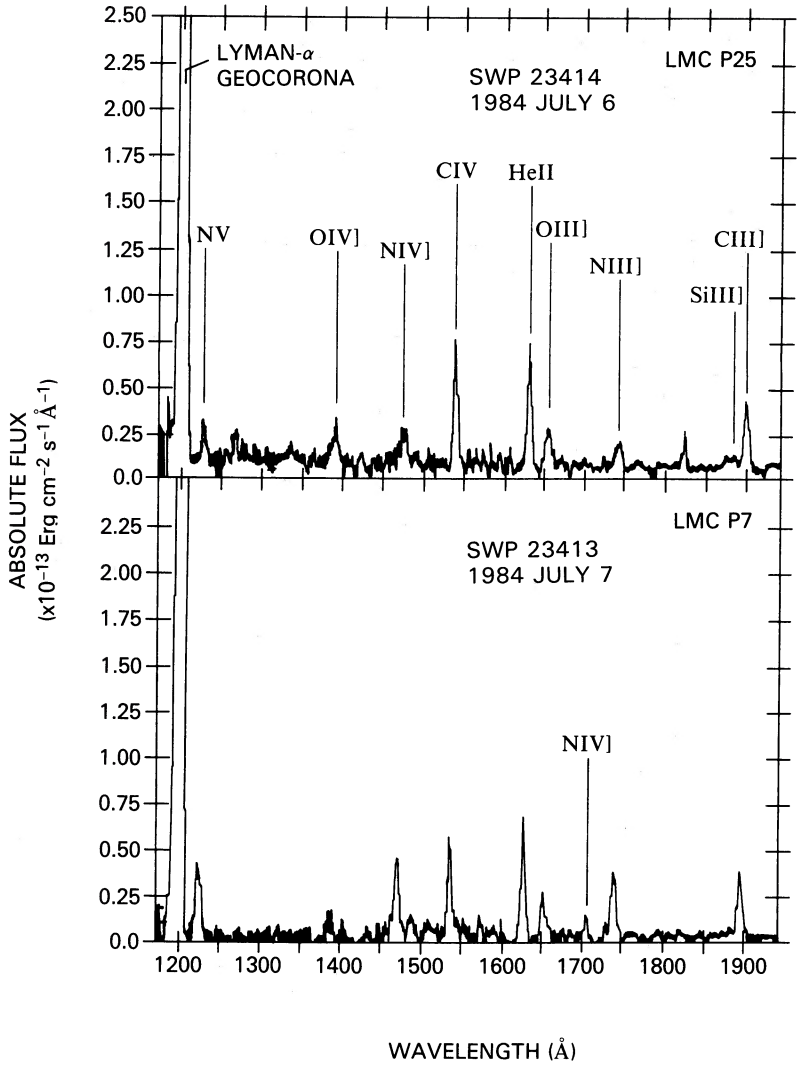

FIG. 3.—Spectrum of LMC P25 and LMC P7. LMC P25 has a rich spectrum, the visible region of which is characterized by forbidden lines of Fe ions. Note the prominence of nitrogen ions in P7.

TABLE 4

OBSERVED UV FLUXES AND CORRECTED INTENSITIES FOR SMALL MAGELLANIC CLOUD

ION	WAVELENGTH (λ)	f_λ	N02		N05		N44	N67	
			Flux	I	Flux	I	Flux	Flux	I
N V	1238.8, 1242.8 1397.2	5.50	...	...	<0.027	<0.135	...	0.30	0.843
O IV	1399.8, 1401.1 1404.8, 1407.4	4.35	...	...	<0.052	<0.186	...	0.06	0.136
N IV	1486.5	3.90	...	...	<0.094	<0.295	...	0.015	0.312
C IV	1548.2, 1550.7	3.60	1.5	1.60	0.88	2.53	0.20	0.13	0.256
He II	1640.3	3.24	0.33	0.36	0.165	0.426	...	0.30	0.551
O III]	1660.8, 1666.2 1746.8	3.15	0.06	0.065	0.061	0.154	...	0.09	0.163
N III]	1748.6, 1749.7 1752.2, 1759.0	2.88	...	...	...	...	...	0.135	0.232
C III]	1906.8, 1909.7	2.37	1.3	2.37	1.08	2.16	1.69	0.055	0.086
Ne IV	2426	1.15	...	...	...	...	...	0.04	0.05
C(UV)	...	...	0.013	...	0.127	0.00	...	(0.00)	0.082

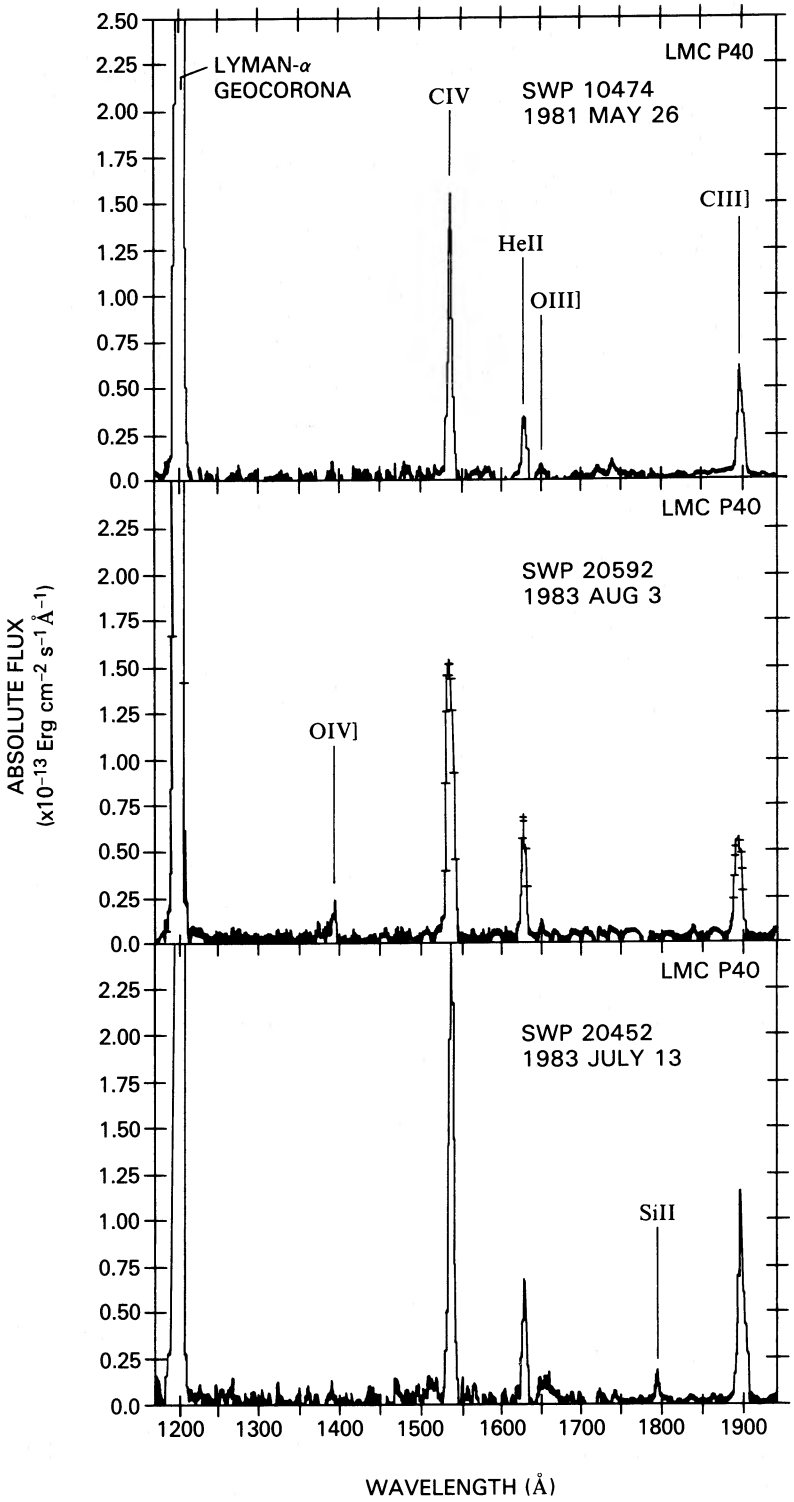

FIG. 4.—Spectrum of LMC P40. Three exposures, SWP 14074, 90 minutes; SWP 20592, 420 minutes; and SWP 20452, 90 minutes, are compared. The strong lines of C IV, C III, and He II are saturated in the long exposure which brings up the weak [O IV] and other features.

If we can trust the plasma diagnostics, particularly T_e, we can calculate ionic concentrations from the observed line intensities. To obtain the total elemental abundances, some procedure must be used to account for the concentrations in unobserved stages of ionization. Often ad hoc empirical formulae are used. Another procedure is to use theoretical nebular models. One either represents the spectral line intensities in detail or obtains a reasonable fit for the line intensities and level of excitation and then uses the model to determine ionization correction factors. The former method is to be preferred for symmetrical nebulae where a wealth of observational data is at hand. For Magellanic Cloud planetaries where little if any nebular structural information is available, the latter procedure offers advantages.

a) Stellar Model Atmospheres

To calculate a model planetary nebula suitable for interpreting measurements of nebular emission lines, it is first necessary to adopt a model for the emergent flux distribution of the central illuminating star. Procedures adopted by various authors include the use of (1) blackbody flux distributions, (2) theoretical fluxes from model atmosphere calculations, and (3) ad hoc modifications to theoretical flux distributions, adjusted to obtain consistency between observed and modeled nebular line fluxes. In earlier work, we have used the stellar model flux distributions of Cassinelli (1971), Hummer and Mihalas (1970), and of Kunasz, Hummer, and Mihalas (1975). These models were calculated for effective temperatures around 100,000 K, 62,000 K, and 48,000 K. They do not always provide satisfactory fits to the ionizing continua of planetary nebula central stars as implied by the line spectra of the nebulae. Accordingly, we investigated the use of new non–LTE plane-parallel model atmospheres by Kudritzki and his associates (Husfeld *et al.* 1984) calculated with the following values of effective temperature and surface gravity: ($T_{\rm eff}$, log g) = (50,000, 3.8): (75,000 4.7): (85,000, 4.72): (85,000, 5.22): (100,000, 5.0): (100,000, 5.5): (115,000, 5.25): (115,000, 5.75). Even this excellent assemblage of models does not constitute a sufficiently fine grid in $T_{\rm eff}$ and log g to represent the spectra of many PN. It has proved necessary often to interpolate between existing models.

A significant characteristic of the Husfeld *et al.* models is that the He II absorption edge at λ228 in the emergent flux distribution weakens with increasing $T_{\rm eff}$ and decreasing log g, and it may even become an emission edge. Consequently, for a given $T_{\rm eff}$, the flux beyond the Lyman limit is much greater than the flux in the corresponding spectral region that is predicted by an LTE model or by a blackbody approximation to the stellar flux distribution. Thus there are profound differences in the ionizing radiation field between the Husfeld *et al.* models and other commonly used models. The present results indicate that the ionizing continua predicted by the Husfeld *et al.* models are more consistent with the nebular emission lines observed in some of our sample of high-excitation planetary nebulae than are those predicted by earlier models.

b) Nebular Model Calculations

We estimate excitation levels from the observed line intensity ratios, [O III] $\lambda\lambda$(4959 + 5007)/[O II] λ3727 and He II λ4686/He I λ5876. Then models are fitted by adjusting the parameters discussed below and requiring that a satisfactory one shall predict the electron temperature implied by the observed ratio, $\lambda\lambda$(4959 + 5007)/λ4363, of the [O III] lines and that it shall predict intensities in the other observed emission lines that are in fair-to-reasonable agreement with observation. We adopted distances of 45.7 kpc and 63.1 kpc for the Large and Small Magellanic Clouds, respectively (Conti, Garmany, and Massey 1984). It is recognized that there is "considerable dispute even over the distance to the LMC" (Cook, Aaronson, and Illingworth 1986). The quoted authors list recent determinations that differ by up to 0.45 mag in the distance modulus. The distances of Galactic planetaries are generally much more uncertain than are those of the Magellanic Clouds. The chemical abundances that we determine here are not very sensitive to the assumed nebular distances; however, other important parameters, such as nebular and stellar masses and luminosities, are obviously sensitive to the adopted distances.

We adopt the basic atomic parameters (photoionization cross sections, recombination and charge exchange coefficients, collision strengths, A values) as compiled by Mendoza (1983) and by Aller (1984) and given in references therein quoted.

Adjustable parameters in the nebular and stellar models are: radius of the central star, stellar emergent flux distribution, nebular chemical composition, geometrical structure, gas density, and truncation radius. We adopted the stellar emergent flux distribution from the model atmosphere chosen; in some cases, it was necessary to interpolate between the tabulated stellar flux models in order to obtain a satisfactory fit. For example, for N44 in the SMC we interpolated fluxes for $T_{\rm eff}$ = 62,500 K.

The necessary condition for an acceptable fit is that the theoretical nebular model gives a good representation of the observed line intensities and of the observed Hβ flux as corrected for interstellar extinction. Let us assume that such a nebular model can be found. Then given the distance of the PN, the flux distribution of the central star, and the cutoff radius or optical depth at the Lyman limit, τ(Lyc), the observed flux in Hβ will permit us to determine $L_{\rm UV}$ (the total ultraviolet luminosity beyond the Lyman limit) and fix the stellar radius.

The Husfeld *et al.* stellar flux models, calculated for a grid of $T_{\rm eff}$ and log g, appear to provide a satisfactory set of starting data. If the adopted stellar flux distribution permits us to obtain by this procedure a nebular model that predicts the observed line intensities, we have confidence in going ahead. In essence, our procedure amounts to an extension of the classical Zanstra technique where the H and He I and He II lines were considered. We attempt to account for the ionization distribution pattern and line intensities of other elements as well. Given these stellar flux models we found we could fix $T_{\rm eff}$ to $\pm$5000 K, employing spectroscopic data from both *IUE* and optical regions. We emphasize that the desired effective temperatures, stellar radii, $L_{\rm UV}$, and eventually core radii, are dependent on these stellar flux models. They will be modified when improved stellar atmospheric and emergent flux models become available.

We found that most of the nebulae appear to be density-limited, rather than photon-flux–limited. If the objects were full Strömgren spheres, low-excitation lines would be much stronger than observed. The cutoff radius (or τ[Lyc]) appears to be well defined. The procedure is to find a nebular model and truncation radius (or τ[Lyc]) that fits the observations. Then we adjust the adopted radius of the star until observed and predicted Hβ fluxes are equal. Thus, L(UV) is precisely defined. The derived L(UV) would be smaller for the full Strömgren sphere situation by an amount ranging from approximately 10% for most LMC planetaries to approximately 45% for the extreme case of P40. In summary, since the distance of the PN

is known, and τ(Lyc) is determined, the observed Hβ flux suffices to determine the total UV luminosity beyond the Lyman limit L(UV) and to fix the stellar radius. The nebulae are assumed to be spherically symmetric. Structures considered are spheres of uniform density, relatively dense shells surrounding a low-density spherical core, or a systematic dependence of density on distance from the center. In the absence of observations of the [O II] λ3726/3729 ratio, we must use density discriminants such as the [S II] λ6717/λ6730 ratio or even the less satisfactory [O II] 3727/7319+7330 ratio. As noted above, the [S II] diagnostic may actually refer to knots of dense filaments, "condensations," ionization edges, etc., rather than to the mean density of the nebula. Fortunately, Michael Barlow was able to supply us with electron density determinations for most of our objects. For P25 and P33 we chose $N_\epsilon = 7150$ and 9200 cm^{-3}, based on Aller and Czyzak (1983) and Aller (1983), respectively. P25 is of interest because of the great strength of forbidden iron lines as compared with ordinary PN, but the great strength of [O II] λ3727 speaks in favor of it being a planetary nebula rather than a symbiotic star. We cannot exclude the possibility that there exists a symbiotic star within a planetary nebula.

The atomic constants and basic physical relationships are "hard wired" into the program initially, but the adjustable parameters are at the disposal of the operator. The program proceeds step-shell by step-shell outward from the central star. The change in the radiation field, distribution of atoms among different ionization stages, the energy balance, the electron temperature, and the line emissivities are evaluated at each point. At several selected radii (one of which can be chosen as the truncation radius), the program prints out the Hβ flux, intensities of various emission lines relative to Hβ, and other information such as the flux in the continuous spectrum due to the free-free and bound-free emission of H, He I, and He II, and the two-photon H continuum.

The distribution of atoms for each element according to ionization stage is computed not only for each shell but also as an average over the total nebular volume bounded by the truncation radius. We determine for each ionization stage, i, of element E, the quantity $x_i = N_i(E)/N(E)$. Set $N_0(E)/N(\mathrm{H}^+) = \sum N_i(E)/N(\mathrm{H}^+)$ where the summation is taken over all *observed* ionization stages of element E. Then the abundance is given by

$$N(E)/N(\mathrm{H}^+) = N_0(E)/N(\mathrm{H}^+)[1/\sum x_i]$$
$$= (\mathrm{ICF})N_0(E)/N(\mathrm{H}^+) ,$$

where ICF is the ionization correction factor. Here, $\sum x_i$ is calculated using values of x_i from the model.

The mean electron temperatures are calculated for each ion by weighting the emissivity in each line at each radial step by the corresponding electron temperatures

$$\langle T_e \rangle_{\mathrm{ion}} = \frac{\sum T_e E_{\mathrm{ion}}(\lambda)}{\sum E_{\mathrm{ion}}(\lambda)} .$$

Table 5 summarizes some characteristics of the models. The columns list as follows: column (1), the name of the nebula; column (2), a serial number identifying the adopted nebular model (in some cases, several models were computed); column (3), the logarithm of the surface gravity and column (4), the effective temperature of the adopted Husfeld *et al.* stellar model atmosphere; column (5), the adopted density (N_{H}) of the model nebula (atoms cm^{-3}); column (6), the radius of the stellar photosphere (R_*) in units of the solar radius and column (7), the ionizing flux ($L_{\mathrm{UV}}[*]$) of the star beyond the Lyman limit in units of the solar bolometric luminosity. After a number of preliminary trials with spherical models, we decided to use the approximation of a single shell surrounding an inner volume of low density. Column (8) gives the inner, or "cut on," radius of this shell in parsecs; column (9) gives the corresponding cutoff radius of the nebula (R_{neb}) in parsecs; column (10) gives the radius in parsecs of the full Strömgren shell for which the nebular size would be limited by the photon flux rather than by the material it contains; column (11), the logarithm of the Hβ flux expressed in ergs cm^{-2} s^{-1} as predicted by the model; column (12), the observed logarithmic Hβ flux, corrected, of course, for interstellar extinction; column (13), the predicted [O III] temperature; column (14), the observed [O III] temperature; column (15) gives the nebular mass (in solar units) derived from the preceding data.

The nebular radii and masses in columns (8), (9), (10), and (15) depend on the assumed distances of the Magellanic Clouds. For the LMC and SMC we assumed distance moduli, $m - M$, of 18.3 and 19.0, respectively (Conti, Garmany, and Massey 1984). If the uncertainties in the distances of the two clouds are respectively of the order of 15% and 25%, then the estimated masses will be uncertain by the order of 35%–60%, respectively, from this cause alone. A further complication arises from the possibility that the material is distributed in a highly nonuniform density pattern. With dense blobs and a small filling factor, a given Hβ flux could be produced by a much smaller total mass than if the N_ϵ distribution is uniform. Remember that the observed Hβ flux must be reproduced; however we manipulate the assumed density distribution or adjust the nebular radius.

The Hβ luminosity L(Hβ) is found by integrating the Hβ emissivity per cm^3 over the entire H II volume of the nebula, thus: $L(\mathrm{H}\beta) = \alpha_{\mathrm{H}\beta} h\nu_{\mathrm{H}\beta} \int N(\mathrm{H}^+)N_\epsilon dV$ or alternatively as $L(\mathrm{H}\beta) = \int 10^{-25} E_{4,2}{}^0 N(\mathrm{H}^+)N_\epsilon dV$ where the integration is taken over the volume, V, $\alpha_{\mathrm{H}\beta}$ is the recombination coefficient for processes resulting in the emission of Hβ and $E_{4,2}{}^0$ is a parameter amounting to 1.24, 0.863, and 0.660 for $T_\epsilon = 10{,}000$, 15,000, and 20,000 (see, e.g., Aller 1984). If the nebula consists of a zone or regions of uniform density occupying a fraction, ϵ, of the total physical volume, then the nebular mass varies as $M_{\mathrm{neb}} \sim N(\mathrm{H}^+)\epsilon[1 + 4N(\mathrm{He})/N(\mathrm{H})]V$. Putting in numerical values, the nebular mass may be computed from the relation

$$M_{\mathrm{neb}} = 0.1035 N_{\mathrm{H}} R_{\mathrm{neb}}{}^3 [1 + 4N(\mathrm{He})/N(\mathrm{H})]\epsilon ,$$

where M_{neb} is given in solar units N_{H} is the total number of H atoms (neutral or ionized) per cm^3, and the nebular radius is in parsecs. Here ϵ is the filling factor taken as 1.0 for spheres; for shells, the appropriate value is easily calculated.

Consider the influence of the adopted density on the mass of the nebula. For a spherical, homogeneous nebula, the change in radius of the ionized volume as N_ϵ is replaced by N_ϵ' would be

$$\log (R'/R) = -\tfrac{2}{3} \log N_\epsilon'/N_\epsilon ,$$

and $M_{\mathrm{neb}}'/M_{\mathrm{neb}} = N_\epsilon/N_\epsilon'$. Thus do inaccuracies in N_ϵ estimates enter directly into errors in the derived masses of the nebular shells. Errors in N_ϵ of the order of 15% to 25% are easily possible for nebulae near the limits of the range over which the 3729/3726 criterion is applicable.

The mean values of the nebular masses in Table 5 are

$$\langle M_{\mathrm{neb}} \rangle_{\mathrm{LMC}} = 0.35 \pm 0.15 \quad \text{and} \quad \langle M_{\mathrm{neb}} \rangle_{\mathrm{SMC}} = 0.29 \pm 0.09 .$$

TABLE 5

SUMMARY OF DATA FOR MAGELLANIC CLOUD PLANETARIES

NEBULA (1)	MODEL NO. (2)	LOG g (3)	$T_{\rm eff}$ (4)	$N_{\rm H}$ DENSITY (5)	$R(*)$ (6)	$L_{\rm UV}(*)$ (7)	INNER RADIUS (8)	CUT-OFF RADIUS (9)	FULL STRÖMGREN SPHERE (10)	$F(\rm H\beta)$ pred (11)	$F(\rm H\beta)$ obsd (12)	T_e ([O III]) pred (13)	T_e ([O III]) obsd (14)	$M_{\rm neb}$ (15)
						SMC								
N2	B11	5.25 Ku	103,750	2850	0.14	5933	0.0490	0.1024	0.1166	−12.68	−12.67	13940	13800	
N5	B1	5.0 Ku	100,000	3900	0.11	3465	0.0495	0.0742	0.0803	−12.91	−12.83	13716	13760	0.17
N43	B4	3.8 Ku	50,000	8000	0.72	7414	0.0455	0.0667	0.0737	−12.41	−12.34	12168	12380	0.24
N44	B3	4.72 Ku	62,500[a]	4200	0.32	5541	0.545	0.0868	0.0968	−12.64	−12.52	11839	12180	0.30
N54	B13	3.8 Ku	50,000	4000	0.62	5510	0.016	0.0226	0.0232	−12.42	−12.42	11960	12000	0.03
N67	B2	5.15 Ku	115,000	3900	0.11	5275	0.0615	0.0906	0.0982	−12.82	−12.84	24022	17500	0.33
						LMC								
P02	S6	5.15 Ku	100,000	3600	0.15	6283	0.0635	0.1009	0.1071	−12.30	−12.33	14258	14560	0.41
P07	S3	5.25 Ku	115,000	2130	0.09	4173	0.0745	0.1208	0.1295	−12.58	−12.58	19125	20300	0.48
P09	S3	5.25 Ku	115,000	7000	0.09	4202	0.0315	0.0502	0.05661	−12.69	−12.72	19400	19800	0.12
P25	S1	5.25 Ku	100,000	7000	0.21	11440	0.0495	0.0855	0.0886	−11.97	−12.01	16610	16900	0.52
P33	S3	4.89 Ku	92,500[a]	9200	0.21	8179	0.0395	0.0606	0.0633	−12.16[a]	−12.19	14290	13920	0.23
P40	S3	5.19 Ku	105,000[a]	1930	0.13	5133	0.0605	0.1153	0.1455	−12.63	−12.69	15570	15820	0.36

[a] Interpolated.

These estimates are rough and will be improved as more nebulae are observed with the speckle interferometric technique. With an SMC distance of 57.5 kpc, $\langle M_{\rm NEB}\rangle_{\rm SMC} = 0.24\ M_\odot$.

c) *Comparison of Theory with Observations*

Table 6 illustrates a typical fit between computed and observed emission line intensities for two planetaries in the LMC. For each emission line in P33 and P40, we give the line identification, wavelength, observed intensity corrected for extinction (see Aller [1983] for the optical region data), and the intensity computed from the adopted model. The intensities are normalized relative to $I(\mathrm{H}\beta) = 100$. Some additional parameters of the respective models, and the Hβ line fluxes corrected for interstellar extinction, are also given. In practice, we first try to fit the [O III] $\lambda\lambda(4959+5007)$/[O II] λ3727 line ratio and then the He II λ4686/He I λ5876 ratio. The degree to which the [O III]/[O II] ratio is matched by the models is shown at the bottom of Table 6. Because of the finite difference character of the calculation, a precise fit is not possible. We also give the values of observed and predicted electron temperatures, the nebular truncation radius, the corresponding optical depth at the Lyman limit ($\tau_{\rm H}$), and the optical depth corresponding to the full Strömgren sphere, $\tau_{\rm FSS}$. The observed line intensities are accurate to about 10% for the strongest lines and are less accurate for weaker lines; for lines with intensities of 5% to 20% of Hβ, the intensities should be good to about 20%, while for lines with intensities of about 1% of Hβ, the errors are about 50%.

The comparison of observed and modeled line intensities often reveals difficulties in predicting lines emitted by ions of the $3p^3$ configuration, e.g., [S II] and [Ar IV] emissions. These inconsistencies may be due to unmodeled density fluctuations such as discrete condensations within a nebula, but they may arise in part from inadequate atomic parameters for the $3p^3$ configuration. Discordances between predicted and observed electron temperatures are sometimes encountered with the present method. For example, when the He II λ4686/He I λ5876 line ratio is well matched, there is a tendency for the predicted electron temperature to be too high. The same discrepancy can occur if the adopted stellar temperature is too high. Of course, we can always lower T_ϵ by introducing a coolant. Dust can be important in real planetaries. In this context, note that in P33 (Table 6), the predicted strengths of the C IV lines are too great, while the opposite applies to P40. Theoretical models sometimes predict systematically too strong C IV lines. Since resonance photons may be repeatedly scattered before they escape, presence of dust can reduce the intensity of C IV (see, e.g., Harrington *et al.* 1982); alternatively, a shell model will predict a similar effect (Köppen and Wehrse 1983).

The pointlike nature of the Cloud planetaries introduces difficulties. Note that lines of ionic N may be at least partially produced by the atmosphere of the central star. We have no means of separating nebular and stellar spectra. This problem of unscrambling stellar and nebular spectra is more tractable in extended galactic planetaries, where it is possible to obtain spectra of regions that exclude the central star. However, in

TABLE 6

REPRESENTATION OF LINE INTENSITIES IN TWO LMC PLANETARIES

		P33		P40	
ION	λ	I_0	Model	I_0	Model
He I	5876	11.8	11.7	5.1	5.1
He I	4471	4.5	4.4	1.9	1.9
He II	4486	30.5	32	64.4	65.9
	4267	1:	0.24	0.35	0.16
C III	1909	815	1026	963	1081
C IV	1549	289	804	1837	1422
[N II]	6583	40.3	41.3	4.1	6.0
[N II]	5755	1.55	1.8		
N IV	1488	...	...	<85	17.1
N V	1239	416	3.6	<41	8
[O II]	3727	64.9	62.6	22:	29
[O II]	7319, 7330	9.7	15.3		
[O III]	4959, 5007	1795	1981	1180	1280
[O III]	4363	21.8	25.7	18.5	19.4
O III	1663	78.1	58	73	51.1
O IV	1403	...	...	<98	76.5
[Ne III]	3868	97.5	103.7	47.9	66.1
[Ne IV]	4726	...	...	1.3	0.6
[Ne IV]	2422	...	...	107	67.8
[S II]	6717	2.1	2.2	1.0	1.0
[S II]	6730	4.7	3.8	1.45	1.4
[S III]	6312	2.4	3.9	1.5	1.9
[Ar III]	7135	10.5	12.8	6.1	8.2
[Ar IV]	4740	4.9	4.5	5.9	4.9
[Ar V]	6435	0.56	0.87		
	7005	1.17	1.9	1.9	4.4
5959+5007/3727	...	28	26.7	53.6	44
T_ϵ	...	13920	14290	15820	15570
r (cutoff)	...	...	0.06056	...	0.11527
$\tau_{\rm H}$	...	...	18.9	...	3.92
τ(FSS)	...	...	107.4	...	93.9

TABLE 7

DETERMINATION OF ELEMENTAL ABUNDANCES IN THE SMALL MAGELLANIC CLOUD

					N2							N5			
Ion	λ	I	T_e	$N(X_i)$	Adopt $\Sigma N(X_i)$	Adopted ICF	ICF Method	Model	I	T_e	$N(X_i)$	$\Sigma N(X_i)$	ICF	ICF Method	Model
He I	4471	3.8		0.081					3.6		0.077				
	5876	10.9	13,760	0.087	0.110	1.0	0.110	0.112	11.5	13,760	0.092	0.123	1.0	0.123	0.123
He II	4686	29		0.256					41		0.036				
C III	1909	847	13,840	2.43(-4)	3.70(-4)	1.146	4.23(-4)	4.5(-4)	1395	13,760	4.14(-4)	6.82(-4)	1.18	8.05(-4)	7.50(-4)
C IV	1549	987	14,640	1.27(-4)					1630	14,120	2.68(-4)				
N II	6584	8.1	13,460	8.08(-7)	8.08(-7)	32.3	2.6 (-5)	2.7(-5)	25	13,600	2.41(-4)	2.4 (-6)	12.2	2.93(-5)	3.30(-5)
N IV	1483,87								<190	14,160	<2.3 (-4)				
N V	1341								< 87	14,760	<5.3 (-5)				
O II	3727	24.5	13,760	4.04(-6)					80	13,800	1.45(-5)				
O III	4959														
	5007	1142	13,760	1.24(-4)	1.28(-4)	1.18[2]	1.53(-4)	1.48(-4)	1293	13,760	1.41(-4)	1.55(-4)	1.20	1.86(-4)	2.20(-4)
O III	1663	45		2.0 (-4)					99	13,800	4.33(-4)				
O IV	1403								<120	14,460	<1.93(-4)				
Ne III	3868	49.8	13,600	1.69(-5)	[1.69(-5)]	(1.35)	2.3 (-5)		87	13,760	2.84(-5)				
Ne IV	4725	0.25	15,400	0.70(-5)	3.06(-5)	1.01	3.15(-5)	2.15(-5)	0.43	14,310	1.86(-5)	5.46(-5)	1.014	5.54(-5)	4.71(-5)
Ne V	3427	< 8.2	15,750	1.87(-6)					32	15,560	7.59(-6)				
S II	6717,30	3.6	13,500	5.98(-8)	6.38(-7)	2.71	1.73(-6)	2.4 (-6)	8.6	13,760	1.59(-7)	1.59(-7)	32.2	5.12(-6)	7.0 (-6)
S III	6312	0.78	13,500	5.78(-7)											
Ar III	7135	4.9	13,500	2.41(-7)	7.85(-7)	1.16	9.14(-7)	8.5 (-7)	7.1	13,760	3.37(-7)	7.83(-7)	1.13	8.85(-7)	1.0 (-6)
Ar IV	4740	3.2	13,500	5.44(-7)					2.6	13,760	4.46(-7)				
He I	4471	5.55							5.0		0.105				
	5876	14.2			0.113	1.0	0.113	0.118	14		0.109	0.108	1.0	0.108	0.117
He II	4686	0.3 (stellar?)							1.5 (stellar?)		0.001				
C III	1908	426		2.45(-4)	2.45(-4)	1.35	3.31(-4)	3.8(-4)	536		3.41 (-4)	3.72(-4)	1.054	3.92(-4)	9.80(-4)
C IV	1549								63		0.314(-4)				
N II	6563	11.7		1.49(-6)	1.49(-6)	27.8	4.14(-5)	4.3(-5)	8.9		1.12 (-6)	1.12(-6)	28.6	3.2 (-5)	3.0 (-5)
O II	3727	14.4		5.36(-6)	1.14(-4)	1.0	1.14(-4)	1.17(-4)	255		7.54 (-6)	1.74(-4)	1.0	1.74(-4)	1.80(-4)
O III	4959														
	5007	751		1.09(-4)					1100		1.66 (-4)				
Ne III	3868	34.8		1.60(-5)	1.60(-5)	1.0256	1.64(-5)	1.65(-5)	76		3.71 (-5)	3.71(-5)	1.015	3.77(-5)	3.90(-5)
S II	6717,30	1.17		4.02(-8)	9.21(-7)	2.30	2.12(-6)	2.3 (-6)	1.5		3.77 (-8)	3.77(-8)	91	3.42(-6)	5.0 (-6)
S III	6312	0.87		8.41(-7)											
Ar III	7135	3.2		1.87(-7)	2.80(-7)	1.0	1.80(-7)	5.0 (-7)	3.2		1.93 (-7)	4.74(-7)	1.0	4.74(-7)	4.70(-7)
Ar IV	4740	0.42		9.3 (-8)					1.17		2.81 (-7)				

TABLE 7—*Continued*

	N67[a]								N54						
Ion	λ	I	T_ε	N_i	$\Sigma N(X_i)$	ICR	ICR Method	Model	λ	I	$N(X_i)$	$\Sigma N(X_i)$	ICF	ICR Method	Model
He I	5876	13.7D 10.8	27,500	0.096 [0.121]	0.149 [0.18]	1.0	0.149 [0.18]	0.20	4471 5876	5.0 15.1	0.104 0.107	0.106	1.0	0.106 ±0.002	0.113
He II	4686	64 D 58	27,500	0.0530 [0.0583]											
									1909	495	3.57(-4)	3.57(-4)	1.385	4.94(-4)	4.70(-4)
C III	1908	65.1	28,640	0.823(-6)	1.53 (-6)	1.22	1.87(-6)	3.04(-6)							
C IV	1549	194	30,030	0.704(-6)											
N II	6563	204	25,650	7.0 (-6)											
N III	1750	176	26,700	1.39 (-5)	2.65 (-5)	1.025	2.72(-5)	4.5 (-5)	6584	3.8	6.83(-7)	6.83(-7)	18.5	1.26(-5)	1.20(-5)
N IV	1483,7	236	30,355	5.6 (-6)	or		or								
N V	1240	639	31,600	4.22 (-6)	3.07 (-5)	1.0	3.1 (-5)								
O II	3727	1.1D 44	25,300	1.77 (-6) [4 (-8)]					3727	4.5	5.36(-6)				
O III	1663	123	27,500	1.75 (-5)	1.135(-5)	1.238 or	1.41(-5)		4959 +5007	544	8.91(-5)	9.45(-5)	1.0	9.5 (-5)	1.00(-4)
O III	4959 5007	347	27,500	0.959(-5)	[0.96 (-5)] or 1.39 (-5)	1.022	[1.19(-5)] or 1.42(-5)	1.7 (-5)							
O IV	1403	103	31,440	2.54 (-6)	[1.21 (-5)]		[1.24(-5)]								
Ne III															
Ne IV	2426	37.9	31,225	8.03 (-7)	8.03 (-7)	4.31	3.46(-6)	8.0 (-5)	3686	19.1	9.77(-6)	9.77(-6)	1.02	1.0 (-5)	1.0 (-5)
S II	6717	14 D	27,500	[2.25 (-7)]	2.25 (-7)	7.41	1.67(-6)	2.6 (-6)	6717,6750	0.45	5.25(-8)	5.25(-8)	67	3.5 (-6)	4.0 (-6)
	6730	205 D													
Ar III									7135	1.04	6.46(-8)	6.46(-8)	2.6	1.68(-7)	1.6 (-7)

[a] In N67 intensities denoted by "D" are from Dufour and Killen (1977); values given in column (4) are from Osmer (1976) and the present paper. Ionic concentrations found with Dufour and Killen data rather than with Osmer's optical region data are given in brackets. Because of the weakness of O IV λ1403 we give two sets of data for oxygen. The upper set, which is obtained by omitting the O IV data, is deemed the more reliable. The N V λ1240 line may be of stellar origin in this nebula. Two values of N(N) are given; the upper is obtained by assuming λ1240 is of stellar origin.

some cases, e.g., LMC P25 (which appears to have strong forbidden iron lines [Aller and Czyzak 1983]), there is good agreement with the observed intensities of ionic N lines. Tables 7 and 8 present our detailed model calculations.

We have used shell models as being more physically realistic than spherical models. Surrounding an inner low-density (100 atoms cm^{-3}) sphere is a uniform shell of density N_H chosen to produce the required N_ϵ value. More elaborate and physically correct models can be calculated when results of the speckle interferometry become available.

Of these objects, SMC N67 is perhaps the most engaging. Its high T_ϵ and abnormal N/O ratio was revealed in the investigations by Osmer (1976) and by Dufour and Killen (1977); more extensive spectroscopy of the visual region is needed.

IV. CHEMICAL COMPOSITION OF THE NEBULAE

Chemical compositions of nebulae can be estimated in two obvious ways. In the first, we adopt the abundances derived from the modeling procedure in which the best fit of predicted-to-observed line intensities is obtained. In the second, we use the "best fit" model nebulae to find the ionization correction factors. In the latter case, abundances are calculated from ICFs together with ionic concentrations derived from observed line intensities and standard formulae (Osterbrock 1974; Aller 1984), given the electron temperature and electron density. The direct-fit or "model" method can be used for symmetrical objects of known structure where detailed observations are available, e.g., IC 3568 (Harrington and Feibelman 1983).

In Tables 7 and 8 we list for each nebula the identification and wavelength of each observed emisson line that was used in the abundance determinations: the observed line intensity, corrected for interstellar extinction, normalized to $I(H\beta) = 100$ and in succeeding columns the adopted electron temperatures, the ionic concentration $N(X_i)$, normalized to $N(H^+)$, the summation of that quantity, $\sum N(X_i)$ over all observed stages of ionization, the adopted ICF, the elemental abundance found from the above-described ICF method, and the elemental abundance derived in the nebular model-fitting procedure. For a number of nebulae, the anticipated T_ϵ differs from ion to ion. For most nebulae, the theoretical model is used as a guide to assign temperatures appropriate for strata of different excitation. When a seemingly reliable T_ϵ can be found from [N II] 6583 and 5755, we use that value for [N II] and [S II]. Generally, the models are not successful in predicting large differences between $T_\epsilon(N^+)$ and $T_\epsilon(O^{++})$. In N43 and N44, uniform electron temperatures of 12,380 and 12,180, respectively, appear to suffice. Table 9 gives the adopted logarithmic nebular abundances.

A kind of self-consistency check on the plausibility of the derived abundance may be found from an examination of the "discrepancy":

$$\Delta = \log N(\mathrm{ICF}) - \log N(\mathrm{model}) .$$

For helium, the mean value, $|\Delta| = 0.02$, shows an agreement that is to be expected since both He I and He II are observed. For other elements, we find that the two abundance procedures yield results differing as shown in Table 10 when averaged over the nebulae in each cloud. In N67 where Ar is not observed, the model fails to reproduce the very high T_ϵ involved and the available optical region data are discordant. We emphasize that the Δ's are not measurements of errors in the derived abundances but indicate how closely the two procedures are in accord.

The mean discrepancies Δ_E between abundance determinations by the two methods averaged over all elements for the SMC and LMC, respectively, are as given in Table 11.

A comparison of our abundance results for SMC N2 with those of Barlow *et al.* (1986) shows reasonably good agreement for most elements. Some discordances arise from differences in the values selected for the measured intensities, particularly for carbon. The N abundance is sensitive to the ionization correction factor, which is large for this element, since only [N II] is observed. The ICF is sensitive to the exact value of the truncation point. The abundances of O, Ne, S, and Ar are in general accord.

Let us now consider the individual abundances, element by element. In N67, the discrepancies are dominated by the disagreement in the visible wavelength optical data, so that nebula is excluded from the following comments. *Carbon.*—The worst discrepancies in the C abundances derived by the two methods are ~ 0.26 in SMC N44 and LMC P7. If observed and predicted C III λ1909 intensities are fitted in N44, $I(1550)$ C IV is observed to be about 5 times too weak, possibly due to internal dust extinction. In P7, the discrepancy is smaller but here $I(1549)$ is larger. *Nitrogen.*—Some large discrepancies are found in the N abundance determinations for LMC P9, P25, and P40. These are probably due to central star contamination of the lines of higher ionic stages; it is difficult to extrapolate the N abundance from observations of [N II] alone. *Oxygen.*—The good agreement in the O abundance determinations from the two methods can be ascribed to the circumstance that most of the atoms occur in the observed O^+ and O^{++} stages. We generally have excluded λ1663 from considerations of the O^{++} ionic abundance determination, since the upper level of this transition may be at least partly populated by dielectronic recombination (Rubin 1986). Hence, abundances derived on the assumption of purely collisional excitation will be systematically too high. At the present time it is not possible to estimate the size of this effect. *Neon.*—In the PN of the present sample, most Ne atoms are in the Ne^{++} stage. The abundance is readily extrapolated from $N(Ne^{++})$ by appropriate ICF factors. The weak, uncertain [Ne IV] lines invariably yield $n(Ne^{+++})$ concentrations that appear too large. Lines of [Ne V] are most useful as indicators of nebular excitation level. *Sulfur.*—The predictions for this element are obviously subject to uncertainty. Only two low ionic stages, S^+ and S^{++}, are observed, and the intensities of the corresponding emission lines are generally reproduced poorly by the models. If the [S II] intensities are represented, that of [S III] is often poorly predicted. The fraction of S concentrated in S^{++} is always much larger than that in S^+. However, the determination of the $N(S^{++})/N(H^+)$ ratio depends on the weak auroral-type line [S III] λ6312 and is very sensitive to the adopted electron temperature. This may help explain the above-noted discordances. It would be very desirable to observe the nebular type 9069, 9532 [S III] lines. *Argon.*—Except for SMC N43, the Ar abundances seem to be relatively well established, depsite possible uncertainties in the atomic data for $3p^2$ and $3p^3$ ions.

The adopted logarithmic abundances for the planetaries in the Small and Large Magellanic Clouds are given in Tables 9*a* and 9*b*. The abundance data for the H II regions in both clouds are from Dufour, Shields, and Talbot (1982) and from Aller, Keyes, and Czyzak (1979). Column (9) of Table 9*a* gives solar abundances of C, N, and O from Lambert (1978) and for the other elements from a compilation by Aller (1986). The solar

TABLE 8

DETERMINATION OF ELEMENTAL ABUNDANCES IN THE LARGE MAGELLANIC CLOUD

		P02							P07						
Ion	λ	I	T_e	$N(X_i)$	Adopt $\Sigma N(X_i)$	Adopted ICF	ICF Method	Model	I	T_e	$N(X_i)$	$\Sigma N(X_i)$	ICF	ICF Method	Model
He I	4471	3.8		0.0825					5.0						
	5876	10.3	14,560		0.112	1.0	0.112	0.115	12.56		0.110	0.160	1.0	0.160	0.161
He II	4686	33.2		0.0295					54.3		0.050				
C III	1908	1076	14,560	2.31(-4)	3.97(-4)	1.15	4.57(-4)	4.2 (-4)	296	20,300	1.28(-5)	1.80(-5)	1.225	2.20(-5)	2.6 (-5)
C IV	1549	1686	15,240	1.66(-4)					394	21,900	5.19(-6)				
N II	6583	33.8	10,860	2.9 (-6)	2.9 (-6)	12.5	3.62(-5)	3.75(-5)	516	119,00	6.62(-5)				
N III	1750								293	20,300	7.0 (-5)				
N IV	1783,87								386	21,000	4.3 (-5)	1.96(-4)	1.0	1.96(-4)	2.3 (-4)
N V	1240								509	22,500	1.73(-5)				
O II	3727	71.3	14,560	1.08(-5)					118	18,700	7.64(-6)				
O III	1663	139		4.27(-4)	1.38(-4)	1.146	1.58(-4)	1.66(-4)	179	20,300	8.89(-5)	0.66(-4)	1.208	8.1 (-5)	9.2 (-5)
	4959 +5007	1341		1.27(-4)					1275	20,300	5.9 (-5)				
Ne III	3868	64.4	14,560	1.77(-5)	1.77(-5)	1.77(-5)	2.27(-5)	2.45(-5)	94	20,300	1.09(-5)	2.33(-5)	1.095	2.55(-5)	1.88(-5)
Ne IV	4726								3.05	22,300	1.24(-5)				
S II	6717,30	10.7	10,860	3.21(-7)	1.66(-6)	1.95	3.24(-6)	4.5 (-6)	63.0	11,960	1.28(-6)	2.47(-6)	1.522	3.76(-6)	4.6 (-6)
S III	6312	2.3	14,560	1.34(-6)					4.92	20,300	1.19(-6)				
Ar III	7135	7.81	14,560	3.34(-7)					14.0	19,400	3.73(-7)				
Ar IV	4740	3.7	14,560	7.09(-8)	9.52(-7)	1.025	9.75(-7)	9.50(-7)	9.54	21,400	6.03(-7)	1.12(-6)	1.048	1.17(-6)	1.20(-6)
Ar V	6435, 7005	1.1	15,760						5.68	22,475	1.36(-7)				
He I	4471	4.15		0.0924					4.4						
	5876	15.3	19,800	0.132	0.173	1.0	0.173	0.195	10	16,900	0.090				
He II	4686	65.7		0.0605					24.1		0.022				
C III	1908	425	20,500	1.77(-5)	2.46(-5)	1.233	3.03(-5)	4.0 (-5)	107	16,900	1.06 (-5)	1.624(-5)	1.146	1.86 (-5)	1.70(-5)
C IV	1549	480	21,500	6.9 (-6)					177	18,400	5.64 (-6)				
N II	6583	354	13,940	3.47(-5)	2.9 (-6)		1.81(-4)	2.4 (-4)	25.6	16,100	1.88 (-6)				
N III	1750	443	20,555	9.75(-5)	1.79(-4)	1.01			51.2	16,900	2.915(-5)	4.68(-5)	1.0	4.68 (-5)	3.7 (-4)
N IV	1483,87	726	21,800	6.79(-5)					51.2	18,800	1.032(-5)				
N V	1240	1380	22,500	4.68(-5)					90	20,400	5.41 (-6)				
O II	3727	72	18,500	7.57(-6)					46	16,100	6.58 (-6)				
O III	1663	194	19,800	1.08(-4)	7.15(-5)	1.34	9.57(-5)	9.8 (-5)	56.5	16,900	7.14 (-5)	1.052(-4)	1.013	1.066(-5)	1.10(-5)
	4959 +5007	1309	19,800	6.39(-5)					1257	16,900	8.47 (-5)				
O IV	1403								73.5	20,300	1.40 (-5)				
Ne III	3868	85.5	19,060	1.14(-5)					80	16,900	1.45 (-5)		1.067	2.52 (-5)	2.4 (-5)
Ne IV	4726	109	22,400	5.95(-6)	1.74(-5)	1.206	2.10(-5)	1.8 (-5)				2.36(-5)			
	4726	3.1		1.06(-5)					1.51	19,900	9.12 (-6)				
S II	6717,30	32.9	13,940	8.51(-7)	2.17(-6)	2.273	4.93(-6)	9.1 (-6)	10.35	16,150	1.89 (-7)	1.17(-6)	2.294	2.674(-6)	3.0 (-6)
S III	6312	5.3	19,800	1.32(-6)					2.62	16,900	9.77 (-7)				
Ar III	7135	14.5	18,900	4.02(-7)					9.3	16,400	3.22 (-7)				
Ar IV	4740	12	20,436	7.98(-7)	1.4 (-6)	1.10	1.55(-6)	1.45(-6)	5.31	16,900	5.33 (-7)	9.23(-7)	1.031	9.52 (-7)	9.9 (-6)
Ar V	6435,	8.5	22,440	2.0 (-7)					2.40	20,165	6.8				

TABLE 8 (Continued)

Ion	λ	P33 I	T_e	$N(X_i)$	P33 Adopt $\Sigma N(X_i)$	P33 Adopted ICF	P33 ICF Method	P33 Model	P40 I	P40 T_e	P40 $N(X_i)$	P40 $\Sigma N(X_i)$	P40 ICF	P40 ICF Method	P40 Model
He I	4471			0.0948	0.1218				1.9?						
	5876	11.8	13,920	0.027		1.0	0.122	0.122	5.1	15,820	0.0416	0.100	1.00	0.100	0.103
He II	4686	30.5							64.4		0.0579				
C III	1908	815	13,920	2.275(-4)	2.8 (-4)	1.164	3.26(-4)	4.0 (-4)	963	15,820	1.32 (-4)	2.45(-5)	1.27	3.12 (-4)	3.34(-4)
C IV	1549	288		5.24 (-5)					1837	16,420	1.13 (-4)				
N II	6584	40.3	14,000	3.97 (-6)	3.97(-6)	14.7	5.84(-5)	5.6 (-5)	4.1	15,820	2.95 (-7)	2.95(-7)	47.6	1.405(-5)	2.2 (-5)
N IV	1483,87								<85	16,596	<3.6 (-5)				
N V	1240	416[a]	15,700	1.34 (-4)					<41	17,180	<7.7 (-6)				
O II	3727	64.9	13,920	1.676(-5)					22:	15,820	2.11 (-6)				
O III	1663	78			2.08(-4)	1.183	2.46(-4)	2.30(-4)	72.7	15,820	1.344(-4)				
	4959, +5007	1795		1.91 (-4)					1180	15,820	0.919(-5)				
O IV	1403								<98	16,840	<9 (-5)				
Ne III	3868	97.5		3.07 (-5)	3.07(-5)	1.319	4.05(-5)	4.0 (-5)	47.9	15,820	1.04 (-5)				
Ne IV	2426								107	15,590	1.60 (-5)	2.65(-5)	1.18	3.12 (-5)	3.12(-5)
	4725								1.31	16,620	2.39 (-5)				
S II	6717,30	6.82		1.94 (-7)	1.74(-6)	2.22	3.87(-6)	5.4 (-6)	2.45	15,320	2.9 (-8)	7.16(-7)	3.33	2.39 (-6)	3.16(-6)
S III	6312	2.38		1.55 (-6)					1.5	15,820	6.87 (-7)				
Ar III	7135	10.5		4.87 (-7)					6.1	15,820	2.25 (-7)				
Ar IV	4740	4.93		7.85 (-7)	1.353(-6)	1.04	1.40(-6)	1.40(-6)	5.9	15,820	7.20 (-7)	1.05(-6)	1.12	1.17 (-6)	1.47(-6)
Ar V	7005	1.17	15,220	8.06 (-8)					1.9	16,820	1.08 (-7)				

[a] N v λ1240 is probably mostly of stellar origin in P33.

TABLE 9A

ADOPTED LOGARITHMIC ELEMENTAL ABUNDANCES AND RATIOS IN THE SMALL MAGELLANIC CLOUD ON SCALE log $N(H) = 12.00$

	SMC						SMC H II		MEAN
ELEMENT (1)	N2 (2)	N5 (3)	N43 (4)	N44 (5)	N54 (6)	N67 (7)	REGIONS (8)	SOLAR (9)	PN (10)
He	11.05	11.09	11.05	11.03	11.03	11.17	10.92	11.00	11.00
C	8.74	8.90	8.52	8.40	8.69	6.27	7.16	8.67	8.71
N	7.5	7.17	7.62	7.50	7.10	7.47:	6.53	7.99	8.26
O	8.16	8.27	8.06	8.24	8.00	7.15	8.07	8.92	8.65
Ne	7.38	7.74	7.22	7.58	7.00	6.54	7.48	8.05	8.00
S	6.26	6.71	6.33	6.54	6.55	6.23	6.48	7.23	7.00
Ar	5.93	5.95	5.45	5.67	5.22	...	5.82	6.6	6.48
C/O	+0.58	+0.63	+0.46	−0.16	+0.69	−0.88	−0.91	−0.25	+0.06
N/O	−0.66	−0.80	−0.44	−0.74	−0.90	+0.32	−1.54	−0.93	−0.39

TABLE 9B

ADOPTED LOGARITHMIC ELEMENTAL ABUNDANCES AND RATIOS IN THE LARGE MAGELLANIC CLOUD ON SCALE log $N(H) = 12.00$

	LMC						LMC H II
ELEMENT	P02	P07	P09	P25	P33	P40	REGION
He	11.05	11.21	11.24	11.05	11.09	11.00	10.93
C	8.66	7.34	7.49	7.27	8.51	8.50	7.90
N	7.56	8.30	8.26	7.67	7.77	7.15	6.98
O	8.20	7.91	7.98	8.03	8.39	8.23	8.41
Ne	7.36	7.41	7.32	7.40	7.61	7.49	7.73
S	6.51	6.58	6.70	6.43	6.59	6.38	6.96
Ar	5.99	6.11	6.19	5.98	6.15	6.07	6.24
C/O	+0.46	−0.57	−0.49	−0.76	+0.12	+0.27	−0.51
N/O	−0.64	+0.39	+0.28	−0.36	−0.62	−1.08	−1.08

abundance of argon is poorly established. The last column gives the mean abundance for approximately 100 planetaries that have been analyzed with the aid of models or from ICF factors found from theoretical models (Aller and Keyes 1987). We also compare the logarithmic C/O and N/O ratios for these planetaries with values found for H II regions, the Sun, and the "mean" for galactic planetaries. Table 9*b* gives corresponding data for the LMC planetaries and for H II regions. The number of nebulae in this sample is still too small to deduce much from statistics but broad trends can be identified.

Consider first the SMC. Excluding the unusual object N67, we find that with respect to H II regions C and N are enhanced by an order of magnitude (see Table 12). Ne, S, and Ar are virtually unchanged. Except for C, the abundances in SMC planetaries are all much smaller than in the Sun and Galactic planetaries. For the LMC means we exclude the N-rich PN, P7 and P9. In the LMC the enhancements of C and N with

TABLE 10

VALUES OF Δ AVERAGED OVER ALL NEBULAE FOR INDIVIDUAL ELEMENTS

$\lvert\Delta\rvert$	C	N	O	Ne	S	Ar
SMC[a]	0.05	0.03	0.03	0.03	0.03	0.08
SMC[b]	0.08	0.06	0.04	0.10	0.10	0.08
LMC	0.07	0.09	0.02	0.04	0.14	0.03

[a] Excluding N67.
[b] Including N67.

TABLE 11

VALUES OF $\lvert\Delta\rvert_E$ AVERAGED WITH ALL ELEMENTS

SMC						
Nebula	N2	N5	N43[a]	N44	N67	
Value	0.04	0.06	0.06	0.03	0.18	
LMC						
Nebula	P02	P07	P09	P25	P33	P40
Value	0.04	0.06	0.10	0.04	0.04	0.07

[a] If we exclude Ar, where abundance is poorly determined for N43, then $\lvert\Delta\rvert_E = 0.02$.

TABLE 12

RATIOS OF MEAN SMC AND LMC PN ABUNDANCES TO ABUNDANCES IN H II REGIONS, THE SUN, AND GALACTIC PLANETARIES
$\langle PN\rangle/\langle el\rangle$

Object	C	N	O	Ne	S	Ar
SMC						
H II	30	8	1.2	0.8	1.0	0.8
Sun	1	0.3	0.2	0.3	0.2	0.1
$\langle PN\rangle_{gal}$	0.9	0.2	0.3	0.3	0.3	0.2
LMC[a]						
H II	4	4	1.5	0.8	1.3	0.7
Sun	0.6	0.4	0.2	0.25	0.2	0.3
$\langle PN\rangle_{gal}$	0.6	0.2	0.1	0.3	0.4	0.4

[a] In LMC means we exclude C, N, and O for P7 and P9.

respect to the H II regions amount to approximately a factor of 4; Ne/O, S/O, and Ar/O are essentially the same in the LMC PN and H II regions. Again, the abundances are all smaller than in the Sun and galactic PN.

It appears that the precursors of the Magellanic Cloud planetaries were not sufficiently massive to synthesize elements such as Ne, S, or Ar. The ratios of these elements with respect to H are much smaller than in our own Galaxy. C, N, and O, however, are affected strongly by element-building processes. The values for each PN reflect the scenarios peculiar to that object. P25 (LMC) seems to show low abundances of C, N, and O; this PN is unique in showing strong forbidden iron ionic lines.

Turning to the C/O ratios, note the low values for N67, P7, P9, and P25 as compared with the Sun. In N67 the O, Ne, and C abundances all seem unusually low—a result consistent with the high electron temperature of this object (compare Osmer [1976] and Dufour and Killen [1977]). As for the N/O ratio, there seem to be few objects with values as low as those found in the Sun. In P7 and P9, O and C appear to have been converted into N.

In stars of low-to-medium mass that are customarily regarded as progenitors of planetary nebulae, Iben and Renzini (1983) identified three dredge-up phases. During an early phase of red giant evolution, material processed in the CN cycle during the main sequence or early shell phase is mixed to the surface. Oxygen is not much affected but C is depressed and N is somewhat enhanced. Among the more massive stars of the group, $2.5 < m < 7\ M_\odot$, the second dredge-up is important. CNO cycle products are copiously mixed to the surface resulting in an increase in N and lowering of C and O. Evidently, planetaries of Peimbert's type I such as P7 and P9 are examples of this type of event. They resemble the galactic PN NGC 6537 (Feibelman, Aller, and Keyes 1985). In this object the O depletion is much greater than predicted by the Iben-Renzini theory. The destruction of O may occur more efficiently than we have supposed. On the asymptotic giant branch (AGB) during the terminal phase of the star's life as a thermonuclear source, C, which has been produced in He burning, is mixed outward during thermal relaxation oscillations. The efficiency of this carbon delivery process is enhanced in stars of low initial O/H or Fe/H ratios such as Population II objects. In view of the abundance of C stars in the Magellanic Clouds, the frequency of C-rich PN is not surprising.

A few words of caution concerning the derived abundances: (1) some elements such as C (Greenstein 1981) assumed to be present only in the gas phase may be partially tied up in grains (as is indeed the situation for iron [e.g., Shields 1981], aluminum, and calcium, [e.g., Aller 1984, p.201]); (2) the abundances may be all systematically low if temperature fluctuations in the nebulae are important (Peimbert 1967; Rubin 1969; Dinerstein, Lester, and Werner 1985). If (2) is significant, then the tabulated depletions with respect to the solar abundances may be overestimated by 0.1–0.2 dex. However, the elemental abundance ratios, C/O, N/O, Ne/O, S/O, and Ar/O would be much less affected (cf. Zuckerman and Aller 1986).

Limitations in the precision of our abundance determinations arise also from

1. effects of line intensity errors,
2. effects of errors in the electron temperature and density,
3. nebular model limitations,
4. central star parameters, especially energy flux distribution and stellar radius, and
5. errors in atomic parameters.

The accuracy of a derived ionic concentration is directly proportional to that of the nebular line intensity. Thus, concentrations found from strong lines such as those of C III, C IV, [N II], [O II], [O III], and [Ne III] which yield abundances of C, N, O, and Ne should be good to approximately 10% in a well-observed nebula, as far as this cause is concerned. For ions represented only by weak lines ([S II], [S III], [Ar III], [Ar IV], [Ar V], [Cl III]) the situation is much less favorable. Errors from this cause can range from 15% to 20% for some Ar ions, to 50% for S and Cl ions. Errors in T_ϵ are particularly serious for ions of C^{++}, C^{+4}, Ne^{+3}, Ne^{+4}, and Ne^{+5} as an elementary calculation quickly shows, particularly when T_ϵ is low. The effect of an error in N_ϵ is much less serious except for p^3 ions of S^+, Cl^{++}, and Ar^{+3}. T_ϵ fluctuations exacerbate the problem (cf. above).

Consider model limitations. Even if we knew the stellar flux distribution exactly we still have the question of the geometrical structure. The simplest comparison is between a spherical nebula and a shell. In a specific example, P40, we found that the error in the ICF in going from a shell model to a sphere was less than 10% except for S and N where the differences were of the order of 30%. The difficulty here is extrapolating from ionization stages, N^+ and S^+ or S^{++}, which contribute only a small fraction of the total ions of that element. Clumping and filamentary structures can further aggravate the problem.

Errors in the radius of the central star have negligible effect on the derived abundances, but errors in the energy flux cannot only influence the evolutionary tracks inferred from the data, but by modifying the far-UV flux they can produce serious errors in the predicted ICFs even if we succeed in predicting reasonable intensities with these erroneous fluxes. It is essential to have the observed intensities from the far-ultraviolet through the optical range.

Errors in atomic parameters would appear to be particularly serious in the $3p^n$, particularly $3p^3$ configuration (cf., e.g., Czyzak, Keyes, and Aller 1986).

V. THE STELLAR MODELS AND CONSEQUENCES FOR STELLAR EVOLUTION

According to Paczyński (1971), the more massive the remnant core of the precursor star, the more rapidly will it evolve as the planetary nebula nucleus (PNN). A core of 1 $M_\odot$ would in fact evolve so rapidly that the change in luminosity would be readily apparent within about two decades. Paczyński showed that the mass of the remnant core (central star) is related to its luminosity. His relation can be expressed as follows:

$$\frac{M(\text{core})}{M(\text{Sun})} = 0.17 \times 10^{-4} L_*/L_\odot + 0.52 .$$

To estimate the masses of the central stars in our sample of 11 Cloud planetaries, we use the luminosity beyond the Lyman limit, L_{UV}*, which is only slightly smaller than the total luminosity for such hot stars. The ultraviolet luminosities and masses of the central stars are listed in Table 13. Note that the masses cluster between 0.58 and 0.71, in the range of most observed white dwarf and planetary nebula central star masses in the Galaxy (Koester, Schulz, and Weidemann 1979; Weide-

TABLE 13

ESTIMATES OF CORE MASSES AND MAXIMUM LUMINOSITIES

SMC	$M_c/M_\odot$	$\log L_{max}/L_\odot$	LMC	$M_c/M_\odot$	$\log L_{max}/L_\odot$
N2.....	0.62	4.32	P2	0.63	4.34
N5.....	0.58	4.34	P7	0.59	4.30
N43.....	0.65	4.38	P9	0.59	4.41
N44.....	0.61	4.36	P25	0.71	4.40
N54.....	0.61	4.52	P33	0.66	4.42
N67.....	0.61	4.36	P40	0.61	4.29

TABLE 14

CONTINUUM TIME VARIABILITY ANALYSIS FOR LMC P40

λ bin Å	1981 May ergs cm^{-2} s^{-1} Å^{-1}	1983 Aug ergs cm^{-2} s^{-1} Å^{-1}
1800–1880.....	2.20×10^{-15}	2.34×10^{-15}
1760–1840.....	2.26×10^{-15}	...
1680–1760.....	2.46×10^{-15}	2.74×10^{-15}
1360–1440.....	2.70×10^{-15}	3.18×10^{-15}
1260–1340.....	2.80×10^{-15}	2.41×15^{-15}

mann 1977; Schönberner and Weidemann 1981; Schönberner 1981; Mendez *et al.* 1981). Even if we allow for an error of 5000 K in our estimates of $T_{\rm eff}$, the mass spread is increased to only 0.57 to 0.75. This is contrary to our earlier results for three of the stars (Stecher *et al.* 1982), a circumstance resulting from a difference in the adopted stellar atmosphere models (also see Tylenda 1984). The astrometric mass of Sirius B remains as the most impressive exception to the tendency of white dwarf masses to values around 0.6 $M_\odot$. Table 13 also lists for each star the "maximum luminosity" (L_{max}) defined by Tylenda:

$$\log L_{max}/L_\odot = 4.77 + \log [0.18 \log N_e - (0.27 \pm 0.05)] .$$

We note that in all cases the Tylenda maximum luminosity exceeds L_{UV}* (see Table 5).

The results for the stellar radii, luminosities, and masses are all smaller than those that we derived previously (Stecher *et al.* 1982) for three central stars of the present sample. The earlier results were obtained with Cassinelli (1971) model atmospheres as sources for the stellar emergent flux distributions. Although the presently adopted Kudritzki-type (Husfeld *et al.* 1984) model atmospheres seem to give more reliable results, it should be noted that these models do not allow for curvature in the atmospheric layers of the stars. Presumably, however, in central stars that are rapidly evolving into white dwarfs, the effects of curvature can be neglected because the atmospheric scale height is very small compared to the stellar radius. Of greater concern is the need for further refinements in model atmosphere theory. Some means must be found for handling the effect of stellar winds on the far-ultraviolet radiation field. These effects vary from one PNN to another but *IUE* data do permit us to determine velocities and estimate mass-loss rates for many galactic planetaries.

Since Paczyński's theory indicates that a PNN of one solar mass or more would evolve rapidly, it is of interest to compare 1981 and 1983 observations of the three planetaries P40, N2, and N5. The relevant data for the continuum and the C III and C IV lines are given in Tables 14 and 15, respectively. The continuum arises primarily from the central star and might be expected to show some indication of a very rapid variation. The time constant for changes in the nebular spectrum is anticipated to be much longer. As reference to Table 15 indicates, there is no evidence for any line intensity variability. Clearly, a baseline longer than 2 yr is desirable; the observations should be repeated with new spacecraft in several years.

Support from NASA grant NSG 5358 to UCLA for the pursuit of these endeavors is gratefully acknowledged by L. H. A. and C. D. K. We are indebted to Michael Barlow for supplying preprints and for N_ϵ and T_ϵ data on a number of Magellanic Cloud PN. Mr. Robert L. O'Daniel edited and typed the manuscript carefully and as swiftly as possible.

TABLE 15A

EMISSION LINE FLUX REPEATABILITY[a]

Ion	P40	N2	N5
C III.....	3%	2%	4%
C IV.....	6%	4%	18%

TABLE 15B

RESULTS ON CARBON LINE RATIOS C III/C IV

Year	P40	N2	N5
1981.....	1.15	0.540	0.833
1983.....	1.13	0.582	0.856

[a] Data were calculated from observations taken at intervals of days or hours.

REFERENCES

Aller, L. H. 1983, *Ap. J.*, **273**, 590.
———. 1984, *Physics of Thermal Gaseous Nebulae* (Dordrecht: Reidel).
———. 1986, in *Spectroscopy of Astrophysical Plasmas*, ed. A. Dalgarno and D. Layzer (Cambridge: Cambridge University Press), in press.
Aller, L. H., and Czyzak, S. J. 1983, *Proc. Nat. Acad. Sci.*, **80**, 1764.
Aller, L. H., and Keyes, C. D. 1987, *Ap. J.*, in press.
Aller, L. H., Keyes, C. D., Czyzak, S. J. 1979, *Proc. Natl. Acad. Sci.*, **76**, 1525.
Aller, L. H., Keyes, C. D., Ross, J. E., and O'Mara, B. J. 1981, *M.N.R.A.S.*, **194**, 613.
Barlow, M. J. 1985, *Observatory*, **105**, 155.
Barlow, M. J., Morgan, B. L., Standley, C., and Vine, H. 1986, *M.N.R.A.S.*, **223**, 151.
Cassinelli, J. P. 1971, *Ap. J.*, **165**, 265.
Conti, P. S., Garmany, C. D., and Massey, P. 1984, *Bull. AAS*, **16**, 948.
Cook, K. H., Aaronson, M., and Illingworth, G. 1986, *Ap. J. (Letters)*, **301**, L45.
Czyzak, S. J., Keyes, C. D., and Aller, L. H. 1986, *Ap. J. Suppl.*, **61**, 159.
Dinerstein, H. L., Lester, D. F., and Werner, M. W. 1985, *Ap. J.*, **291**, 561.
Dufour, R. J., and Killen, R. M. 1977, *Ap. J.*, **211**, 68.
Dufour, R. J., Shields, G. A., and Talbot, R. J. 1982, *Ap. J.*, **252**, 461.
Feibelman, W. A., Aller, L. H., and Keyes, C. D. 1985, *Proc. Nat. Acad. Sci.*, **82**, 2202.
Greenstein, J. L. 1981, *Ap. J.*, **245**, 124.
Harrington, J. P., and Feibelman, W. A. 1983, *Ap. J.*, **265**, 258.
Harrington, J. P., Seaton, M. J., Adams, S., and Lutz, J. H. 1982, *M.N.R.A.S.*, **199**, 517.
Henize, K. 1956, *Ap. J. Suppl.*, **2**, 315.
Hummer, D. C., and Mihalas, D. 1970, J.I.L.A. Report No. 101.
Husfeld, R., Kudritzki, R. F., Simon, K. P., and Clegg, R. E. S. 1984, *Astr. Ap.*, **134**, 139.
Hutchings, J. B. 1982, *Ap. J.*, **255**, 70.
Iben, I., and Renzini, A. 1983, *Ann. Rev. Astr. Ap.*, **21**, 271.
Koester, D., Schulz, H., and Weidemann, V. 1979, *Astr. Ap.*, **76**, 262.
Köppen, J., and Wehrse, R. 1983, *Astr. Ap.*, **123**, 67.
Kunasz, P. B., Hummer, D. G., and Mihalas, D. 1975, *Ap. J.*, **203**, 92.
Lambert, D. L. 1978, *M.N.R.A.S.*, **182**, 249.
Maran, S. P., Aller, L. H., Gull, T. R., and Stecher, T. P. 1982, *Ap. J. (Letters)*, **253**, L43.
Mendez, R. H., Kudritzki, R. P., Gruschinske, J., and Simon, K. P., 1981, *Astr. Ap.*, **101**, 323.

Mendoza, C. 1983, *IAU Symposium 103, Planetary Nebulae*, ed. D. R. Flower (Dordrecht: Reidel), p. 143.
Nandy, K., Morgan, D. H., Willis, A. J., Wilson, R., and Gondhalekar, P. M. 1981, *M.N.R.A.S.*, **196**, 955.
Osmer, P. S. 1976, *Ap. J.*, **203**, 352.
Osterbrook, D. E. 1974, *Astrophysics of Gaseous Nebulae* (San Francisco: Freeman).
Paczyński, B. 1971, *Acta Astr.*, **21**, 417.
Peimbert, M. 1967, *Ap. J.*, **150**, 825.
Rubin, R. H. 1969, *Ap. J.*, **155**, 841.
———. 1986, *Ap. J.*, **309**, 334.
Schönberner, D. 1981, *Astr. Ap.*, **103**, 119.
Schönberner, D., and Weidemann, V. 1981, in *Physical Processes in Red Giants*, ed. I. Iben, Jr. and R. Renzini (Dordrecht: Reidel), p. 463.
Seaton, M. J. 1978, *M.N.R.A.S.*, **185**, 5P.
———. 1979, *M.N.R.A.S.*, **187**, 75P.
Shields, G. A. 1978, *Ap. J.*, **219**, 559.
Stecher, T. P., Maran, S. P., Gull, T. R., Aller, L. H., and Savedoff, M. 1982, *Ap. J.* (*Letters*), **262**, L41.
Tylenda, R. 1984, *Astr. Ap.*, **138**, 317.
Weidemann, V. 1977, *Astr. Ap.*, **61**, L27.
Webster, B. L. 1969, *M.N.R.A.S.*, **143**, 79.
Westerlund, B. E., and Smith, L. F. 1964, *M.N.R.A.S.*, **127**, 449.
Zuckerman, B., and Aller, L. H. 1986, *Ap. J.*, **301**, 772.

LAWRENCE H. ALLER and CHARLES D. KEYES: Department of Astronomy, University of California, Los Angeles, CA 90024

THEODORE R. GULL, STEPHEN P. MARAN, and THEODORE P. STECHER: Code 680, NASA-Goddard Space Flight Center, Greenbelt, MD 20771

ANDREW G. MICHALITSIANOS: Code 684, NASA-Goddard Space Flight Center, Greenbelt, MD 20771